CHEMISTRY OF MATERIALS

ARTICLE

pubs.acs.org/cm

Synthesis, Structural Characterization, and Electrical Properties of $(Sr_{0.5}Ca_{0.5})(Ca_{0.5}Sb_{0.5})O_{3-\delta}$ Double Perovskites

B. Moreno,[*,†,‡] E. Urones-Garrote,[§] E. Chinarro,[†] L. Fuentes,[∥] and E. Morán[‡]

[†]Instituto de Cerámica y Vidrio, CSIC, C/Kelsen 5, 28049, Cantoblanco, Madrid, Spain

[‡]Departamento de Química Inorgánica, Facultad de Ciencias Químicas, Universidad Complutense, 28040 Madrid, Spain

[§]Centro de Microscopía y Citometría, Universidad Complutense de Madrid, 28040 Madrid, Spain

[∥]Centro de Investigación en Materiales Avanzados CIMAV, Complejo Industrial M. Cervantes 120, Chihuahua 31109, México

ABSTRACT: Double perovskites which exhibit 1:2 B-site ordering are under focus because of their interesting structure−property relationships and high chemical versatility. Perovskites with a big cation, such as Sr^{2+} or Ca^{2+}, occupying the octahedral B site are very scarce because the calculated Goldschmidt tolerance factor becomes quite small as these types of cations usually occupy the A-site. This work describes the synthesis and structural and microstructural characterization of a new calcium and strontium antimoniate which shows face-centered cubic symmetry and a rock-salt ordered distribution of Sb^{5+} and Sr^{2+}. The ordered-cation distribution occurs due to the differences in both the ionic sizes and the bonding character of the two B-site cations. As a consequence of the cation stoichiometry of the title phase and assuming a pentavalent state for Sb, a large concentration of oxygen vacancies are created ($y \sim 0.25$). Diffraction studies reveal that these vacancies tend to arrange in a short-ordered way and are related to oxygen ionic conductivity (10^{-3} S/cm at 700 °C) which makes these materials potential candidates to be used as electrolytes in solid oxide fuel cells (SOFC).

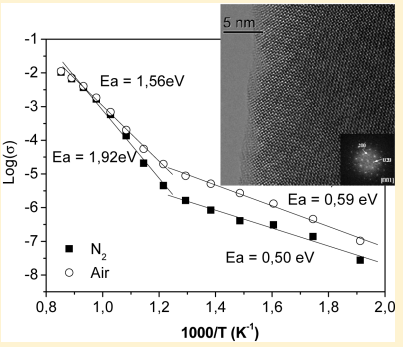

KEYWORDS: double perovskites, antimoniates, electrical conductivity, oxygen deficient perovskites

1. INTRODUCTION

Materials belonging to the ABO_3 perovskite structural type or to closely related structures present many important and valuable technological applications derived from their interesting structure-properties relationships and amazing chemical versatility: for example, see the review by Mitchell.[1] Some of them, showing different ordering in the B-site with two cations with significant charge and/or size differences, are known as double perovskites and are currently attracting much attention. If the Goldschmidt tolerance rules are obeyed, B octahedral sites are occupied only by transition metal cations while bigger cations such as Ca or Sr enter the A cuboctahedral site; thus, perovskites with alkaline-earth cations in the B site are very scarce. The Ca−Sr−Sb−O system was first studied by Blasse,[2] who identified a cubic perovskite, $Sr_3CaSb_2O_9$, with a = 8.17 Å, showing a 1:1 order sublattice of smaller cations. When alkaline elements share the B site with a transition element as Sb^{5+}, electronic and ionic mixed conductivity is expected as a consequence of the creation of oxygen vacancies. Moreover, in previous works[3,4] the preparation of ordered double perovskites of formula $Sr(Sr_{0.5}Sb_{0.5})O_{3-\delta}$ was reported, with face-centered cubic symmetry and $Fm\bar{3}m$ space group. In these materials, a rock-salt ordered distribution of Sb^{5+} and Sr^{2+} on the octahedral sites was found together with a large number of oxygen vacancies. The authors found that the sample exhibited ionic conductivity of 10^{-4} S/cm at 600 °C. In this case B substitution was only considered in order to increase oxygen vacancies in the sample. Earlier works proposed the addition of Ca to promote the synthesis of double perovskites with formula $Sr_{(1.45-x)}Ca_xSb_{0.55}O_{3-y}$,[5] and several compositions were prepared with a cubic symmetry and a cell lattice that decreases when the Ca content increases; nevertheless, the electrical behavior of theses compositions was not tested by the authors. Following these considerations a double perovskite with general formula $Sr_{0.5}CaSb_{0.5}O_{3-y}$ has been synthesized and characterized, finding a noticeable amount of oxygen vacancies (y = 0.25). Two different symmetries have been considered in the crystallochemical studies done, first the $Fm\bar{3}m$ space group for a cubic perovskite with B-cation ordering and second the $P2_1/n$ space group for a monoclinic rock salt ordered perovskite. TEM studies revealed a well ordered structure without extended defects, showing diffuse scattered intensity in the electron diffraction patterns, probably ascribed to the oxygen vacancies generated, which are responsible for the electrical conductivity displayed at moderate temperatures, ∼10^{-3} S/cm at 750 °C.

2. EXPERIMENTAL SECTION

The ceramic conventional method was employed for the synthesis of $Sr_{0.5}CaSb_{0.5}O_{3-\delta}$. High purity precursors $SrCO_3$, $CaCO_3$, and Sb_2O_3 were supplied by Aldrich (>99%) and mixed in the stoichiometric ratio. After grinding, the mixture was first calcined at 800 °C in air for 24 h and

Received: October 11, 2010
Revised: January 11, 2011
Published: March 02, 2011

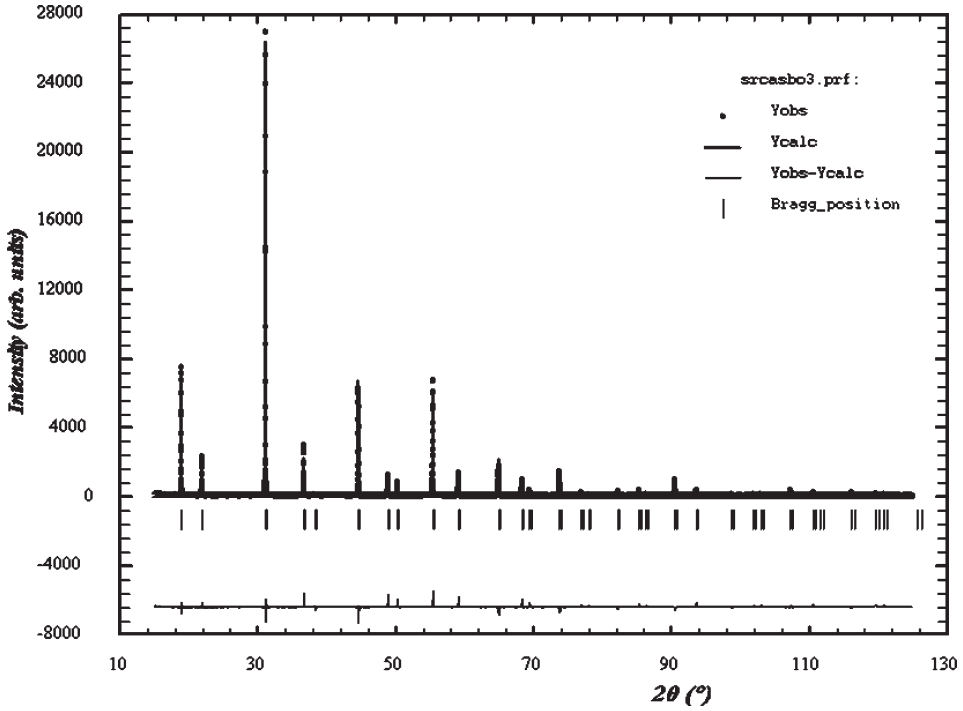

Figure 1. Observed and calculated X-ray diffraction patterns of the sample $Sr_{0.5}CaSb_{0.5}O_{3-\delta}$ after thermal treatment in air at 1200 °C/120 h.

quenched at room temperature. These powders were reground, pelleted, and calcined again at 1200 °C for 120 h. After each thermal treatment the pellet was quenched, reground, and characterized by X-ray diffraction (XRD). Phase identification was performed employing XRD with a XPERT-PRO, the wavelength employed was $K\alpha_1$ λ = 1.540560 Å, the angular domain was $10 \leq 2\theta \leq 125$, and size step $(2\theta) = 0.0084°$. Crystal structure analysis was resolved via Rietveld analysis of X-ray powder diffraction, employing the Fullprof[6] software. Morphological and microstructural characterization of the powders was performed by means of transmission electron microscopy (TEM). Selected-area electron diffraction (SAED) and microdiffraction patterns were acquired in a JEM 2000FX microscope, analyzed with an EDS (energy-dispersive spectroscopy) microanalysis system. High-resolution TEM (HRTEM) images were recorded in a JEM 3000F microscope, operating at 300 kV with a point resolution of 1.7 Å. Specimens for TEM observations were prepared from ultrasonically dispersed suspensions of the sample in *n*-butanol. Several drops of the suspension were dropped on a copper grid covered with a holey carbon film. Electrical properties were measured by electrochemical impedance spectroscopy with Agilent 4294A equipment; measurements were performed in air and N_2 in the frequency range from 40 Hz to 10^7 Hz and varying the temperature from 200 °C to 900 °C. The data were analyzed using a nonlinear least-squares fit method refined by the Boukamp software.

3. RESULTS AND DISCUSSION

The solid state reaction between the reactants at 1200 °C can be expressed as

$$CaCO_3 + 0.5SrCO_3 + 0.25Sb_2O_3 + (0.75 - \delta) / 2O_2(\text{air}) \rightarrow Sr_{0.5}CaSb_{0.5}O_{3-\delta} + 1.5\,CO_2(g) \qquad (R1)$$

The synthesis in air of the sample led to a white powder that showed an XRD pattern characteristic for the perovskite-related structure, Figure 1. The quantitative elemental analysis of the powders, obtained by EDS, showed a cationic ratio of metals consistent with the nominal composition proposed. $Sr_{0.5}CaSb_{0.5}O_{3-\delta}$ was obtained as a single-phase as shown in Figure 1; the reflections indexed in the X-ray pattern are consistent with a cubic perovskite cell structure, ascribed to a face-centered lattice with a space group *Fm*3*m*. Nevertheless, this XRD pattern matches some other related perovskites described in the literature that crystallizes with different symmetry. For this reason, another space group apart from *Fm*3*m* was considered for Rietveld refinement.

3.1. Structure of $Sr_{0.5}CaSb_{0.5}O_{3-\delta}$. Luhrs et al.[7] reported the study of double perovskites based on Sr and Ca antimoniates with monoclinic symmetry ($P2/n$); however, this space group was not considered in the present work due to the clear differences found between both XRD patterns and also due to the electron microdiffraction patterns obtained with TEM (see Figure 4). Colomban et al.[8] have proposed a hypothetical structure for cubic perovskites considering structural oxygen vacancies, but their proposal concerns a chain-based structure with the transformation of B octahedra in pyramids as a consequence of the location of the oxygen vacancies. On the basis of this model and a similar one proposed,[9] a tetragonal symmetry has been considered as an alternative to a cubic one; therefore, the Rietveld refinement was also carried out with the *I*4*mm* space group. The crystal rearrangement differentiates mainly two oxygens in the tetragonal lattice. The adjustment was performed without success, as the refinement in the oxygen occupancies was not accurate and resulted in data with no physical sense. For this reason this spatial group was abandoned, and the refinement was done considering the cubic one.

The structure refinement data of $CaSr_{0.5}Sb_{0.5}O_{3-\delta}$ are listed in Table 1. The numbers in parentheses represent standard deviations, and the absence of parentheses means that the considered quantity remained fixed during the refinement. The number of refined parameters (structural and instrumental) was 22. Temperature factors did not show stability during refinement; consequently, these parameters were fixed, and the overall temperature factor was refined in a value of B_{over} = 2.416(9). Final disagreement factors were R = 15.8 and χ^2 = 7.73, which

dx.doi.org/10.1021/cm1029276 |*Chem. Mater.* 2011, 23, 1779–1784

Table 1. Crystal Structure of $Sr_{0.5}CaSb_{0.5}O_{3-\delta}$ Space Group *Fm*3*m* Cell Parameters Obtained from the Rietveld Refinement[a]

atom	site	*x*/*a*	*y*/*a*	*z*/*a*	occup.	B_{iso} (Å)
O	24e	0.218(5)	0	0	18	0.000
Sr(1)	8c	1/4	1/4	1/4	4	0.000
Ca(1)	8c	1/4	1/4	1/4	4	0.000
Sb(1)	4a	0	0	0	4	0.000
Ca(2)	4b	1/2	1/2	1/2	4	0.000

[a] a = 8.1200(1) Å, S.G. = *Fm*3*m* (No. 225), Z = 8.

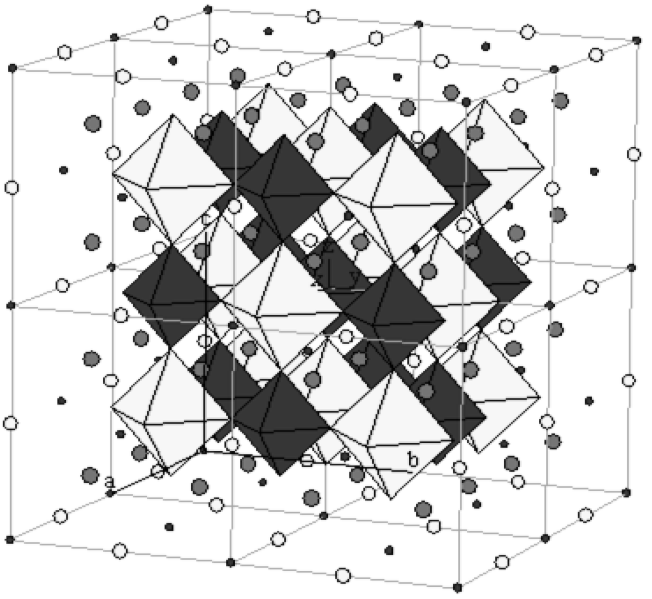

Figure 2. Crystal structure of $Sr_{0.5}CaSb_{0.5}O_{3-\delta}$ showing a rock salt ordering. Spheres: large white → Sr; small black → Sb; large gray → Ca. O atoms at the corners of Sb/Ca-coordination octahedra omitted.

indicates a good agreement between the experimental and calculated XRD patterns as a satisfactory convergence was reached.

In Figure 2, a scheme of the investigated structure (*Fm*3*m*) is depicted. It can be observed that in this perovskite the lattice parameter was doubled, finding a = 8.1200(1) Å. The doubling of the perovskite is known to be associated with the differences in size and or charge of the cations located in the B-site. Although in this case the introduction of Ca in the lattice, both in A and B sites, produces a lower lattice parameter than that reported by others.[3,5] The structure shows evidence of B-cation order, as the lattice parameter is doubled and the (111) reflection is clearly indexed in the XRD pattern (Figure 1).[10] B-sites of the structure are occupied 50% by Ca and 50% by Sb; these octahedra show significant differences in the M−O (M = Sb and Ca) bond lengths, and these differences are related with the atomic radius of both atoms, rCa^{2+} = 1.14 and rSb^{5+} = 0.74, as shown in Figure 3. Therefore, after the Rietveld refinement this composition can be reformulated as $(Sr_{0.5}Ca_{0.5})(Ca_{0.5}Sb_{0.5})O_{3-\delta}$.

It was previously demonstrated that antimony appears as Sb^{5+} in this type of material. In early works published by the group it was also determined that there was one type of oxygen coordination around Sb^{5+}, and in the same way in the present work the number per formula unit of oxygen vacancies, calculated considering electroneutrality of the material, is 0.25.[4] These oxygen

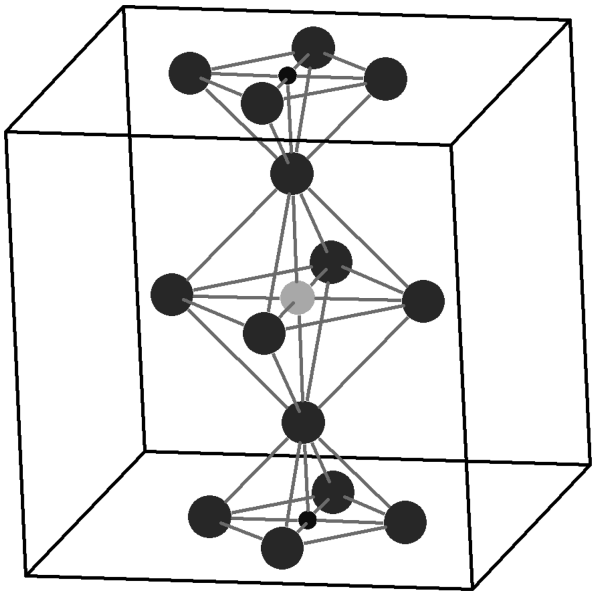

Figure 3. $Sr_{0.5}CaSb_{0.5}O_{3-\delta}$ unit cell showing a rock salt ordering. Spheres: large, gray → O; small gray → Sb; medium, pale gray → Ca. Differences in d(Ca−O) and d(Sb−O) distances along c axes can be distinguished.

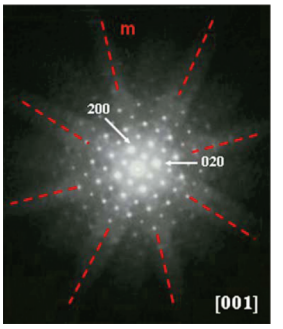

Figure 4. Microdiffraction pattern of $Sr_{0.5}CaSb_{0.5}O_{3-\delta}$ along the [001] zone axis. The mirror planes (m) are marked in the pattern, showing (4*mm*) ideal symmetry.

vacancies are closely related to the ionic conductivity of the perovskite, with the aim of examining oxygen vacancies and determining whether they were ordered, a microstructural study was performed employing electron microscopy. The actual space group can be identified by means of the microdiffraction technique[11,12] by studying the "ideal symmetry" of the microdiffraction patterns, which is determined by the position and relative intensity of the reflections, either on the zero-order Laue zone (ZOLZ) or in the whole pattern, which includes high-order Laue zones (HOLZ).

A microdiffraction pattern from a main zone axis of the structure is shown in Figure 4, which reveals the presence of (4 mm) projection symmetry along the [001] orientation. This is compatible with several tetragonal and cubic space groups, which helps us to confirm the initial refusal of the *P*2/*n* symmetry considered at the beginning on the basis of Luhrs et al. assumptions.[7] In any case, the presence of this axis does not discriminate among the $Fm\bar{3}m$ and the *I*4*mm* groups considered above. In this case, and as shown by Rietveld refinement, the cubic symmetry is the one that succeeds in the adjustment of the XRD pattern.

dx.doi.org/10.1021/cm1029276 |*Chem. Mater.* 2011, 23, 1779–1784

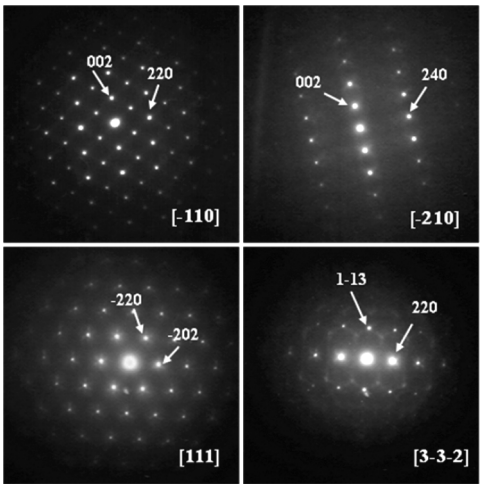

Figure 5. SAED patterns of $Sr_{0.5}CaSb_{0.5}O_{3-\delta}$ oriented along different zone axes, showing diffuse scattered intensity in addition to the basic reflections.

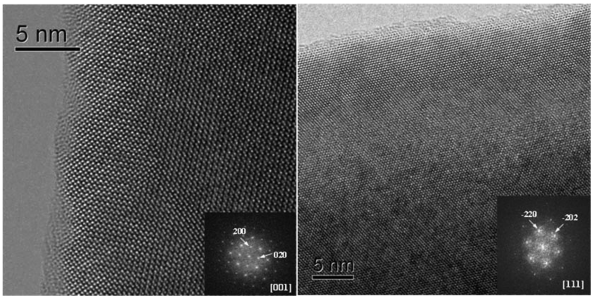

Figure 6. HRTEM images of $Sr_{0.5}CaSb_{0.5}O_{2.75}$ along [001] and [111] orientations.

SAED patterns along different orientations show the presence of diffuse scattered intensity in addition to the basic reflections, as it is shown in Figure 5. This type of effect is often attributed to short-range order phenomena in the structure.[13] In our case, the existence of diffuse scattered intensity between the Bragg spots can be directly related to short-range order in the anion sublattice, that is, the vacancies and the oxygen anions do not dispose totally at random. HRTEM images of the sample (see Figure 6) are typical of well ordered crystals, due to the absence of extended defects. The mottled contrast observed in them confirms the existence of short-range order phenomena in the crystals.

3.2. Electrical Conductivity. The electrical conductivity of $(Sr_{0.5}Ca_{0.5})(Ca_{0.5}Sb_{0.5})O_{3-0.25}$ was studied by AC impedance spectroscopy. For this purpose the material was pressed uniaxially and sintered at 1200 °C/120 h to obtain a compact pellet, and Pt electrodes were painted on both sides; the measurements were carried out both in air and in nitrogen, up to 900 °C. The presence of oxygen vacancies in the perovskite samples is responsible for the ionic conductivity of the material. Nyquist plots (Figure 7) show that the spectra acquired are composed of only one semicircle at low and intermediate temperatures (250−500 °C); this arc, whose resistance decreases with temperature, has been associated with the bulk conductivity of the sample and has been fitted to a equivalent circuit formed by a resistance, in parallel with a CPE (constant phase element), which shows a high depression angle.

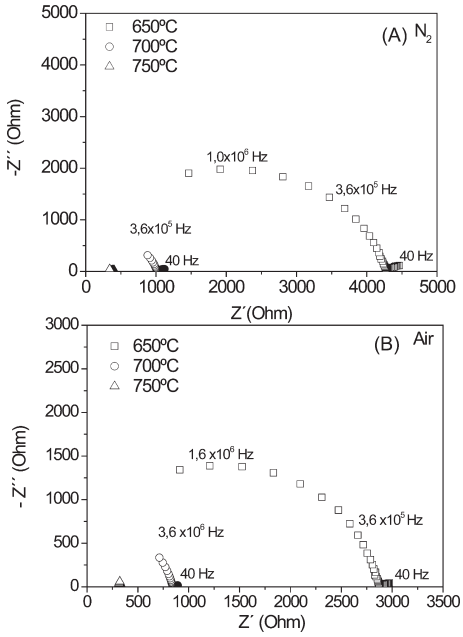

Figure 7. Nyquist plots of measured AC impedance of $Sr_{0.5}CaSb_{0.5}O_{3-\delta}$ at different temperatures in (a) N_2 and (b) O_2 atmosphere.

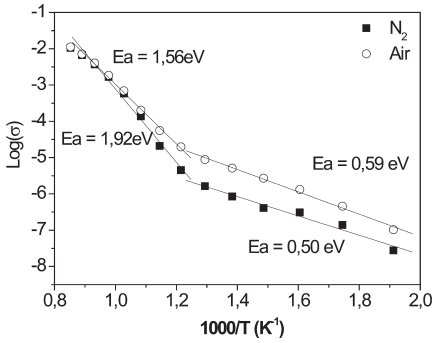

Figure 8. Ahrrenius plots of total conductivity of $Sr_{0.5}CaSb_{0.5}O_{3-\delta}$ in N_2 and O_2 atmospheres.

Similar behavior is found at higher temperatures, with the presence of a second semicircle associated to an interfacial subcircuit, which contains the electrical effect of both grain boundaries and the material-electrode interface, being the total electrical contribution of these phases overlapped. Arrhenius plots ($\log \sigma$ (S cm^{-1}) vs $1000/T$ (K^{-1})) in various atmospheres are shown in Figure 8. A significant reduction of conductivity in N_2 atmosphere (one order of magnitude) has been observed in correlation with previous works, which reported this effect in typical oxygen electrolytes as the result of Coulomb interactions between mobile species.

The conductivity data fit well to the Arrhenius expression $\sigma = \sigma_0 \exp(-E_a/kT)$, where σ is the measured conductivity, σ_0 is a pre-exponential factor, E_a is the activation energy, k is the Boltzmann constant, and T refers to the temperature of the measurements. Two different activation energies were found in the measurements no matter what atmosphere was used. In the range of room temperature to 450 °C, the activation energies measured were 0.50 and 0.60 eV, respectively; these values indicate the dominance of ionic conductivity. The presence of mixed conductivity has been discarded because no Sb^{3+} has been

dx.doi.org/10.1021/cm1029276 |Chem. Mater. 2011, 23, 1779–1784

detected in the samples. Moreover, the structural properties of the material indicate strong difficulties in creating electronic jumps among Sb equivalent sites. On the other hand, from 450 to 900 °C, the conductivity follows a different trend increasing significantly with temperature up to 0.011 S/cm at 900 °C. For the indicated temperature range, the plots show steeper slopes, which implies higher activation energies, 1.56 and 1.92 eV, in O_2 and N_2, respectively. According to the conclusions reached in the structural characterization, this double perovskite contains a large amount of oxygen vacancies (0.25 per mol) that are mainly ordered and probably associated with Ca^{2+} cations. Usually, oxygen vacancies are created by A-site doping, and in our case the amount of Ca in the samples is enough to generate them. The most critical questions that arouse in this type of material are related with the ability of those defects to diffuse in the crystal lattice and the amount of them that can be considered associated to the structure. The electrical conductivity observed in the Arrhenius plots (Figure 8) could explained both questions in close agreement with the structural observations. The lower value of activation energy (0.50 and 0.60 eV, respectively) found suggests a low oxygen vacancy migration at low and intermediate temperatures, and these values are also similar to other classical electrolytes.[14−16] This is indicative, within this temperature range, of a low concentration of free Vö, which should exhibit high mobility (due to the activation energies calculated). As temperature increases, a large energy is required to break down the pairs Vö−Ca^{2+} and also to overcome the Vö ordering, as indicated by the high value of activation energies (1.56 and 1.92 eV) found.

These assumptions are described in other well-known oxygen conductors[17] and, in relationship with the conductivity values found, suggest the existence of an excess of oxygen vacancies, which are prone to generate Coulomb interactions with charged defects and to form clusters blocked in the crystal lattice, as observed in TEM ordering (Figure 5). Nevertheless, these trapped defects are released as temperature increases, and the thermal energy is enough to activate their free motion and, therefore, to increase conductivity at higher temperatures.[18]

Contributions to activation energy can be expressed as $E_T = E_M + E_A + E_{OR}$ where E_M referrers to the migration energy, E_A is a term related to the association of mobile species, and E_{OR} is the energy of Vö ordering.[19] Therefore, the balance of all contributions can be followed in the Arrhenius plots (Figure 8) depicted, and at low temperatures (room temperature to 450 °C) E_A is negligible comparing to the conductivity ascribed to the mobility of species. The influence of this term (E_A) increases with temperature, considering that at higher temperatures more mobile species are created, although they are not available. This fact involves an increase in the E_M and E_{OR} contribution and therefore in the total activation energy, with an enhancement of the ionic conductivity. Related works centered in the characterization of strontium antimoniates reported similar electrical behavior with conductivities in the same range as the ones described in the present work; nevertheless, those materials do not show two different activation energies and, therefore, different conduction mechanisms depending on the temperature.[4] The structural characterization has revealed the presence of a short-range order in the anion sublattice, which could be the answer to the explanation for the electrical behavior of these materials, as it has been reported that well-ordered Vö could lead to a decrease in the anion transport of the material.[20]

4. CONCLUSIONS

The double perovskite with formula $(Sr_{0.5}Ca_{0.5})(Ca_{0.5}Sb_{0.5})O_{2.75}$ has been successfully synthesized as a single phased material. Rietveld refinement has revealed that this material crystallizes with a cubic symmetry in a face-centered lattice with a space group *Fm*3*m*. B site ordering has been established between Sr^{2+} and Sb^{5+}, while the refinement shows that the A position is found totally occupied by Ca atoms. A great number of oxygen vacancies are created in this structure, and diffraction studies have confirmed the arrangement of these defects with a short-ranged ordering which is responsible for the low mobility of this species at intermediate temperatures and, thus, for the electrical conductivity measured in this sample, which is $\sim 10^{-3}$ S/cm at 700 °C. This material seems to be promising as a solid electrolyte as it shows very low electronic conductivity, while a decrease in the vacancy concentration will improve its ionic conductivity.

AUTHOR INFORMATION

Corresponding Author
*E-mail: berta@icv.csic.es.

ACKNOWLEDGMENT

The authors are grateful for the financial support provided by CSIC (PIIs, 200860I130), European Community (UE, FCH-JU-2008-1 No. 245355), Micinn: MAT2010-19837-CO6-03, and Comunidad Autonoma de Madrid, P2009/PPQ-1626, program Materyener2.

REFERENCES

(1) Mitchell, R. H. *Perovskites: modern and ancient*; Almaz Press Inc.: Thunder Bay, ON, Canada, 2002.
(2) Blasse, G. *J. Inorg. Nucl. Chem.* **1965**, *27*, 993.
(3) Saidi, M.; Morán, E.; Amador, U.; Gallardo-Amores, J. M.; Abboudi, M.; Asskali, A. *Int. J. Inorg. Mater.* **2001**, *3*, 1.
(4) Chinarro, E.; Mather, G. C.; Caballero, A.; Saidi, M.; Morán, E. *Solid State Sci.* **2008**, *10*, 645.
(5) Saidi, M.; Morán, E.; Amador, U.; Abboudi, M.; Askali, M. *Mater. Res. Bull.* **2000**, *35*, 1269.
(6) Rodriguez-Carvajal, J. *FULLPROF: a program, for Rietveld refinement and pattern matching analysis*; Abstract of the satellite meeting of the XVth Congress of the International Union of Crystallography, Toulouse, France, 1990; p 127.
(7) Luhrs, C. C.; Beltrán-Porter, D.; Sapiña, L.; Fuertes, A. *Int. J. Inorg. Mater.* **2000**, *2*, 483.
(8) Colomban, P.; Romain, F.; Neiman, A.; Animitsa, I. *Solid State Ionics* **2001**, *145*, 339.
(9) Simon, S. Doctoral Thesis, Universidad Complutense de Madrid, Madrid, 2007.
(10) Anderson, M. T.; Greenwood, K. B.; Taylor, G. A.; Poeppelmeir, K. R. *Prog. Solid. State Chem.* **1993**, *22*, 197.
(11) Spence, J. C. H.; Zuo, J. M. *Electron Microdiffraction*; Plenum Press: New York, 1991.
(12) Morniroli, J. P.; Steeds, J. W. *Ultramicroscopy* **1992**, *45*, 219.
(13) Withers, R. L. Disorder: Structured diffuse scattering and local crystal order. In *Advances in Imaging and Electron Optics*; Hawkes, P. W., Ed.; Academic Press: San Diego, 2008; Vol. 152.
(14) Navarro, L. M.; Recio, P.; Jurado, J. R.; Durán, P. *J. Mater. Sci.* **1995**, *30* (8), 1949.
(15) Hernandez, M. T.; Jurado, J. R.; Durán, P. *Solid State Ionics* **1992**, *51* (3−4), 147.
(16) Sorensen, O. T. *Nonstoichiometric Oxides*; Academic Press: New York, 1981.

(17) Lee, J. S.; Lerch, M.; Maier, J. *J. Solid State Chem.* **2006**, *179* (1), 270.
(18) Valov, J.; Rührup, V.; Rödel, T. C.; Stork, A.; Berendts, S.; Dogan, M.; Wiemhöfer, H. D.; Lerch, M.; Janek, J. *Solid State Ionics* **2009**, *180*, 1463.
(19) Traqueia, L. S. M.; Pagnier, T.; Marques, F. M. B. *J. Eur. Ceram. Soc.* **1997**, *17* (8), 1019.
(20) García-Martín, S.; Fagg, D. P.; Irvine, J. T. *Chem. Mater.* **2008**, *20*, 5933.